

Structure and Energetics of Single-Walled Armchair and Zigzag Silicon Nanotubes

A. S. Barnard[†] and S. P. Russo*

Department of Applied Physics, Royal Melbourne Institute of Technology University, GPO Box 2476V, Melbourne, 3001 Australia

Received: March 24, 2003; In Final Form: May 21, 2003

In past years carbon nanotubes have been the subject of intensive experimental and theoretical efforts, probing their structural, energetic, mechanical, and electronic properties. Recently the successful synthesis of silicon nanotubes (SiNT) has been reported, making these once-hypothetical structures a new candidate for future nanodevices. Presented here is an ab-initio study of the energetics of infinite armchair and zigzag SiNT structures. The zigzag and armchair nanotubes studied here have been structurally relaxed prior to the calculation of the cohesive and strain energy for each chirality. The structural and energetic properties are then discussed. This constitutes part of an ongoing study examining the importance of chirality in the energetic and electronic properties of silicon nanotubes. Understanding the dependence of the properties of silicon nanotubes on their diameters and chirality is important, if they are to be successfully integrated into the nanodevices of the future.

1. Introduction

The discovery of carbon nanotubes (CNT) by Iijima¹ in the early 1990s inspired a new branch in materials science, dedicated to the development of technology at the nanoscale. Numerous studies have been conducted to explore the unique structural to electronic properties of nanotubes,² such as high mechanical strength, high thermal and chemical stabilities, and excellent heat conduction.³ Although CNTs may be readily synthesized using a variety of techniques, only a few nanotubes have been created from materials other than carbon. Success has been achieved with NiCl nanotubes,⁴ Mo and W chalcogenide nanotubes,^{5–7} and B_xC_yN_z composites nanotubes.^{8–10}

To date, theoretical studies have played an important part in the development of the science surrounding nanotubes. The conductivity properties of single-walled carbon nanotubes were predicted theoretically well before experimental observation. These predictions that the electronic properties of nanotubes depend on both the diameter and the chirality of the hexagonal lattice along the tube^{11–13} have since been confirmed experimentally.¹⁴ The structure and energetic properties of CNT^{15,16} have also been found to be affected by length¹⁷ and curvature.¹⁸

Theoretical predictions have also been made of the electronic structure and stability of GaSe,¹⁹ GaN,²⁰ and P²¹ nanotubes, as well as various fullerenic and tubular silicon structures.^{22–24} The ab-initio electronic, structural, and thermal properties of “hypothetical” infinite SiNTs have been compared with CNTs by Fagan et al.^{25,26} More recently, Zhang et al.²⁷ have compared the electronic structure of a finite silicon nanotube with a comparable silicon nanowire and carbon nanotube, while the structure and thermal behavior of silicon nano-cages and nanotubes have been investigated by Kang et al.²⁸ using classical molecular dynamics with the Tersoff potential. The results indicate that, under appropriate conditions, SiNT structures may be stable. Beyond the classical nanotube, silicon nanostructures

are already being proposed as candidates for encapsulation of metals. Ivanovskaya et al.²⁹ have investigated hypothetical SiNTs containing regular chains of metallocarbohedrenes, using a one-dimensional tight-binding model within the Hückel approximation; and Singh et al.³⁰ have investigated the properties of fine, finite, and infinite hexagonal prismatic silicon tubes containing beryllium.

Studies of this type are currently particularly topical, as silicon nanotubes are no longer hypothetical. Sha et al.³¹ have reported the successful synthesis of multiwalled SiNTs using a chemical vapor deposition process, within nanochannels of an Al₂O₃ substrate. These SiNT structures are grown in combination with silicon nanowires and have been characterized using selected-area electron diffraction (SAED) and high-energy transmission electron microscopy (HRTEM). Therefore, the aim of our study is to investigate the effects of chirality and diameter on electronic, structural, and energetic properties of SiNTs, using ab-initio methods. Presented here is a comparison of the energetic and structural properties of armchair and zigzag SiNT structures as a function of tube diameter. This investigation has been designed to determine if energetically preferred chiralities may be expected.

2. Ab-Initio Method

The calculations performed here have been performed with the Vienna ab-initio simulation package (VASP)^{32,33} using ultra-soft, gradient-corrected, Vanderbilt-type pseudopotentials (US-PP)³⁴ as supplied by Kresse and Hafner.³⁵ The crystal relaxations were performed in the framework of Density Functional Theory (DFT) within the Generalized-Gradient Approximation (GGA), with the exchange-correlation functional of Perdew and Wang (PW91).³⁶ The relaxation technique used here is an efficient matrix-diagonalization routine based on a sequential band-by-band Residual Minimization Method of single-electron energies,^{37,38} with direct inversion in the iterative subspace. Both the ionic positions and super-cell volume have been relaxed. Thus, both the symmetry and the lattice parameter are free to change, resulting in expansions or contractions of the entire

* Author to whom correspondence should be addressed. E-mail: salvy.russo@rmit.edu.au.

[†] E-mail: amanda.barnard@rmit.edu.au.

nanotubes. We have successfully applied this technique to the relaxation of bulk diamond,³⁹ nanodiamond,⁴⁰ and fullerene⁴¹ structures in the past, with results giving excellent agreement with experiment and all electron methods.^{35,39}

During initial testing on bulk silicon we have applied the Linear Tetrahedron (LT) method with a $6 \times 6 \times 6$ Monkhorst-Pack k-point mesh, and have expanded the valence orbitals on a plane-wave basis up to a kinetic energy cutoff of 200.00 eV. Using these parameters we calculated a lattice parameter for bulk silicon of 5.456 Å, the sp^3 bond length of 2.362 Å, and the cohesive energy of 4.621 eV. These values are all in good agreement with the experimental values of 5.4309 Å, 2.352 Å, and 4.62 eV, respectively. Therefore, as the SiNT structures are periodic only in the z -direction, we have used a $4 \times 2 \times 6$ k-mesh and 200.00 eV plane-wave cutoff for the remainder of this study. This choice of k-mesh, while containing superfluous k-points in the nonperiodic dimensions, was necessary to stabilize the LT method.

3. Structure and Energetics

The structure of a nanotube may be describe entirely in terms of the length and chirality. The chirality and diameter are uniquely defined in terms of the magnitude of the components of the chiral vector $C_h = n\bar{a}_1 + m\bar{a}_2 \equiv (n, m)$, where n, m are integers and \bar{a}_1, \bar{a}_2 are the unit vectors of a hexagonal, graphene-like sheet. The chiral vector C_h therefore connects two crystallographically equivalent sites on the sheet. The particular chiralities known as “armchair” and “zigzag” are named for the cases where $m = n$ and $m = 0$, respectively. The term “chiral” is used for all other values of m .

In previous studies, only a limited number of SiNT structures have been examined. Fagan et al.²⁶ calculated the properties, of selected zigzag, chiral, and armchair structures, (6,6), (8,2), (6,0), (8,0), (10,0), (12,0), and (14,0), whereas Zhang et al.²⁷ chose only the fine (3,3) armchair structure. Here, we have undertaken a systematic study of silicon in the armchair and zigzag structures with $n = 3$ to 9. Armchair and zigzag SiNTs have been chosen because of their structural simplicity and suitability as limiting cases in a broader study of chiral tubes. Examples of the chosen structures are shown in Figure 1, highlighting the different diameters resulting from the zigzag and armchair configurations for a given value of n .

All SiNTs studied here have been relaxed prior to the calculation of the structural and energetic properties, for each chirality. In the particular case of the (3,0) SiNT, the tubular structure was found to be unstable. The axial length of the nanotube contracted, and the structure puckered to form a single column of diamond-structured silicon with a bond length of 2.306 Å. For this reason, this structure has been ignored in the following analysis.

The bond lengths between neighboring silicon atoms in the remaining structures varied little among the nanotubes, averaging 2.245 Å. This is significantly less than the bulk-silicon bond length of 2.352 Å, as expected, and is in excellent agreement with the values on 2.245 Å calculated by Fagan et al.,²⁵ 2.25 Å calculated by Zhang et al.,²⁷ and 2.305 Å calculated by Kang et al.²⁸ The diameters of 7.48 Å and 9.96 Å for the (6,0) and (8,0) SiNTs, respectively, were however slightly over those reported by Fagan et al. of 7.44 Å and 9.92 Å, respectively.

3.1. Cohesive Energy. Like the bond length, the cohesive energy of silicon in tubular form is expected to differ from that of bulk silicon. Even though both silicon and carbon are isovalent, their chemical behavior is quite different. The sp^2 hybridization is more stable in carbon, whereas the sp^3

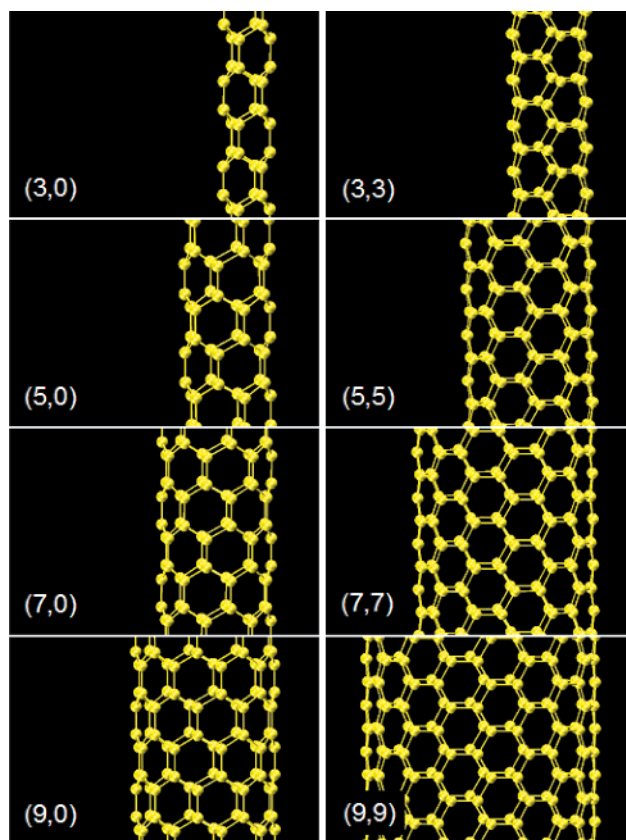


Figure 1. Examples of the relaxed zigzag (left) and armchair (right) silicon nanotube structures, with $n = 3, 5, 7$, and 9 (as marked). Nanotubes with $n = 4, 6$, and 8 , although considered in this study, are not shown.

hybridization is more stable in silicon.⁴² Therefore, while carbon is stable as graphite, fullerenes, and nanotubes (composed of only sp^2 bonds), silicon is traditionally associated only with the diamond structure.

Figure 2 shows the energy per silicon ion as a function of the number of ions (top) and as a function of the nanotube diameter (bottom). It appears from the top graph that the armchair structure has a lower energy than the zigzag structure, for a given number of silicon atoms. However, when the energy is considered as a function of the nanotube diameter, it is clear that this difference is entirely due to the different diameters of each chiral configuration. When the different chirality is accounted for, it appears that the zigzag structure is energetically preferred. Another important feature of Figure 2 is that the energy relationship is nonlinear. This indicates that the cohesive energy is dependent not only on the diameter of the structure, but also on aspects affected by the diameter such as the curvature of the nanotube.

3.2. Strain Energy. To treat the energy associated with the curvature of a SiNT, it is necessary to define a term for this energy that vanishes in the limit as the structure becomes a flat sheet. The continuum treatment used here to describe the strain energy of a nanotube assumes that there are only two in-plane elastic constants, and that the sheet is homogeneous and elastically isotropic. This method has previously been applied to the study of fullerenes.⁴¹ Hence, ignoring higher-order effects such as torsional bending, the deformation energy consists of stretching (first-order) and bending (second-order) terms. In nanotubes, the stretching term is the cohesive energy of the carbon atoms and the bending term provides the strain energy

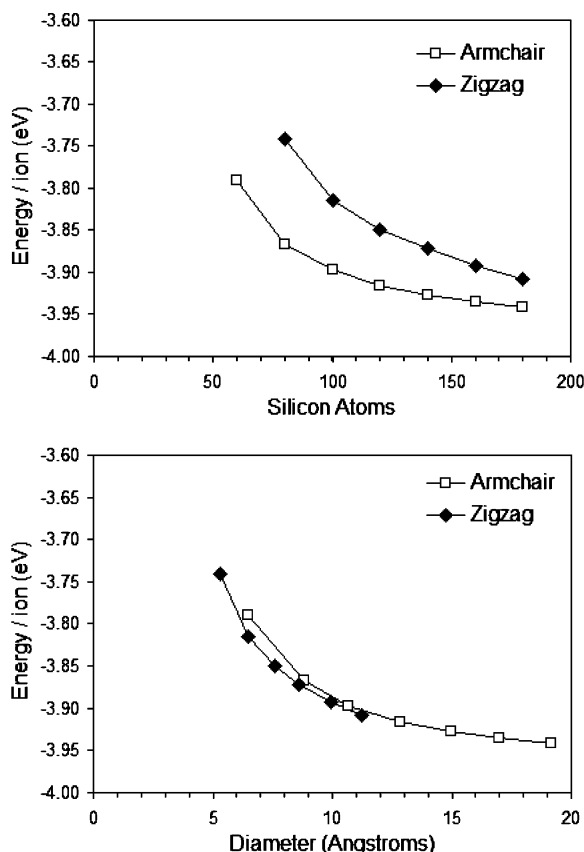


Figure 2. Energy per ion for the SiNT armchair and zigzag structures, as a function of number of atoms (top) and nanotube diameter (bottom). The (3,0) SiNT has been excluded.

associated with curvature of the cylindrical structure:¹⁵

$$E = E_{\text{bend}} + E_{\text{stretch}} = E_{\text{strain}} + E_{\text{cohesive}} \quad (1)$$

Making the assumption that, for the general case, the strain in an elastic cylinder can be modeled by considering the bending and stretching of a suitable elastic sheet, the bending energy (E_{strain}) per unit area (A) is given in terms of the sheet thickness (h) by

$$\frac{E_{\text{strain}}}{A} = \frac{\kappa}{2} \int_{-h/2}^{+h/2} dz \frac{z^2}{R^2} = \frac{\kappa h^3}{24R^2} \quad (2)$$

where κ is the bending modulus of the sheet, and R is the radius of curvature. The strain energy per silicon atom is therefore:

$$\frac{E_{\text{strain}}}{N} = \frac{A\kappa h^3}{N24R^2} \quad (3)$$

For a nanotube, if we assume a cylindrical model, R is also equal to the mean radius, $A = 2\pi RL$, and $N = 2\pi RL\rho$. We have also assumed here that the number density ρ is a constant. This results in an expression for the strain energy per silicon atom, which is linearly dependent on the inverse square of the curvature of the structure:

$$\frac{E_{\text{strain}}}{N} = \left(\frac{\kappa h^3}{\rho 24} \right) \frac{1}{R^2} = E_s \frac{1}{R^2} \quad (4)$$

Note that the coefficient is scaling invariant, and that the strain energy E_s is a constant. This is a suitable definition for use here as E_s may be obtained by fitting the calculated energy to the

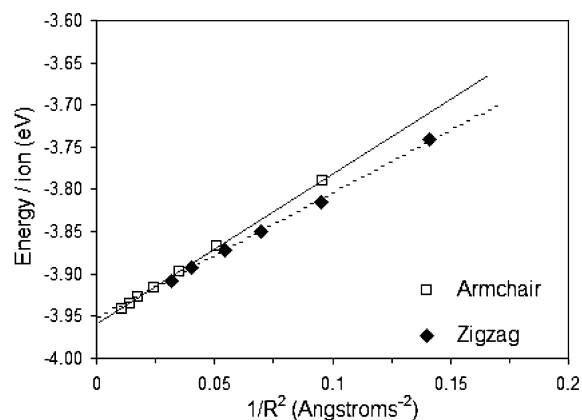


Figure 3. Energy per silicon ion versus the inverse square of the nanotube radius, with the linear fits used to determine the strain energy.

inverse of the square of the SiNT curvature. Hence, the strain energy and cohesive energy may be obtained from the slope and intercept of a linear fit to the energy per ion versus $1/R^2$ respectively, as

$$\frac{E}{N} = E_s \frac{1}{R^2} + \frac{E_{\text{cohesive}}}{N} \quad (5)$$

where E is the total SiNT energy calculated explicitly with DFT.

This relationship is given in Figure 3 for each chirality. From the linear fits, the intercepts give an estimate of the cohesive energy of a flat hexagonal silicon sheet of -3.9596 eV and -3.9543 eV for the armchair and zigzag configurations, respectively. These are both in excellent agreement with the calculated cohesive energy for a hexagonal silicon sheet of -3.9557 eV. The slope of each fit gave a value for the strain energy of 1.782 eV for the armchair structure, and 1.494 eV for the zigzag structure. This indicates that there is more energy required to curve an (n, n) silicon sheet into a nanotube, than an $(n, 0)$ sheet, for the same value of n .

4. Discussion of Results

Although SiNTs have been successfully synthesized, there is no doubt that they are highly metastable structures due to the preference of silicon to be sp^3 hybridized. There is a definite “cost” associated with the forming of a SiNT. Fagan et al.²⁶ showed that while there is cost to produce hexagonal graphene-like sheets of silicon, once they are formed, the extra cost to produce the tubes is of the lower cost than that in carbon. Therefore, the cost of making a nanotube of particular chirality will depend on the strain energy associated with the chirality, as well as the cohesive energy of the corresponding hexagonal silicon sheet.

The method used here to estimate the relative cost of armchair and zigzag SiNTs is to determine the atomic heat of formation, as a function of nanotube size. This technique is based on the model outlined by Barnard et al.,⁴¹ where it was applied to the study of fullerenes. The atomic heat of formation of a silicon nanotube (ΔH_f^0) is expressed in terms of the Si–Si bond energy ($E_{\text{Si–Si}}$) and the strain energy (E_{strain}), such that

$$\Delta H_f^0 = \frac{3}{2} N E_{\text{Si–Si}} + N \Delta H_f^0(\text{Si}) + E_{\text{strain}} \quad (6)$$

where N is the number of silicon atoms, and $\Delta H_f^0(\text{Si})$ is the standard heat of formation of silicon at 298.15 K. Dividing by N gives the atomic heat of formation which has a $1/R^2$

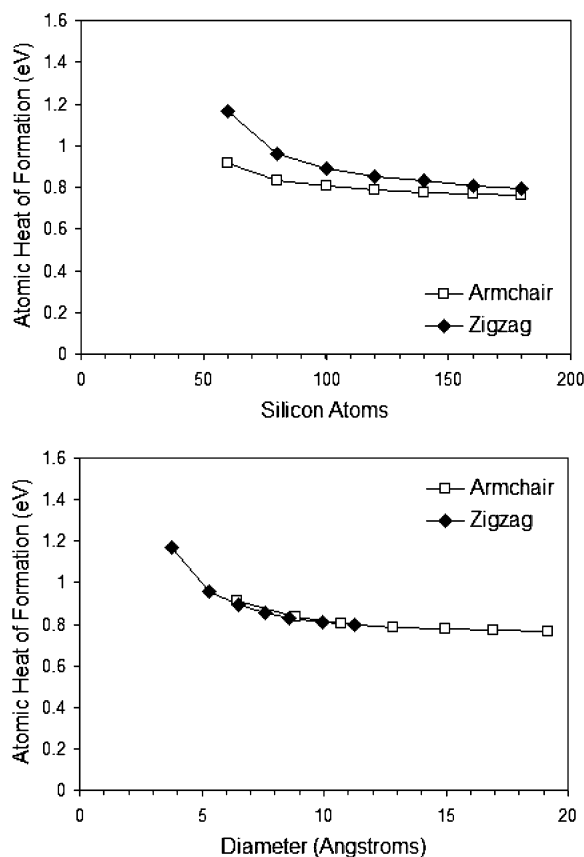


Figure 4. The calculated atomic heat of formation $\Delta H_f^0/N$ as a function of the number of silicon atoms (top) and the nanotube diameter (bottom).

dependence on the strain associated with the curvature of the nanotube:

$$\frac{\Delta H_f^0}{N} = \frac{3}{2}E_{\text{Si-Si}} + \Delta H_f^0(\text{Si}) + \frac{E_s}{R^2} \quad (7)$$

We note that $E_{\text{Si-Si}}$ is calculated at 0 K (using DFT) while $\Delta H_f^0(\text{Si})$ is determined at 298.15 K, but previous calculations performed on carbon have found the temperature dependence of $\Delta H_f^0/N$ to be <0.1 eV, and have therefore been ignored in this treatment.

Therefore, using the cohesive and strain energies for each chirality determined from Figure 3, $\Delta H_f^0/N$ has been calculated for armchair and zigzag SiNTs for the cases $n = 3$ to 9. By plotting this as a function of the number of atoms, the top graph in Figure 4 shows that for a given number of atoms the cost of producing a SiNT is less for an armchair structure than a zigzag structure. However, when $\Delta H_f^0/N$ is plotted as a function of nanotube diameter (bottom of Figure 4), it is clear that this is due to the larger diameter of an armchair structure, and the atomic heat of formation is independent of chirality.

It is also important to note that the atomic heat of formation asymptotes to a finite, positive value, offering further confirmation that a hexagonal graphene-like silicon sheet is not the lowest energy structure for silicon.

5. Conclusions

We have shown here, using ab-initio calculations, that the atomic heat of formation of a silicon nanotube is dependent on the nanotube diameter, but independent of the chiral structure of the tube. It has also been shown that the individual cohesive

and strain energies are dependent on both the diameter and chirality. For example, the strain energy for a zigzag nanotube has been found to be lower than for a corresponding armchair structure, which points to a dependence of the strain energy on m .

The nature of this dependence is currently under investigation for mixed (n, m) chiral structures, as part of an ongoing study examining the importance of chirality in the energetic and electronic properties of silicon nanotubes. Understanding the dependence of the properties of silicon nanotubes on their diameters and chirality is important, if they are to be successfully integrated into the nanodevices of the future.

Acknowledgment. We thank Prof. I. Snook for his helpful advice and comments in the review of this work. This project has been supported by the Victorian Partnership for Advanced Computing and the Australian Partnership for Advanced Computing supercomputer center.

References and Notes

- (1) Iijima, S. *Nature* **1991**, 354, 56.
- (2) Wildoer, J. W. G.; Venema, L. C.; Rinzler, A. G.; Smalley, R. E.; Dekker, C. *Nature* **1998**, 391, 59.
- (3) Saito, R.; Dresselhaus, G.; Dresselhaus, M. S. *Physical Properties of Carbon Nanotubes*; Imperial College Press: London, 1998.
- (4) Hachohen, Y. R.; Grunbaum, E.; Tenne, R.; Sloand, J.; Hutchinson, J. L. *Nature* **1998**, 395, 336.
- (5) Tenne, R.; Margulis, L.; Genut, M.; Hodes, G. *Nature* **1992**, 360, 444.
- (6) Feldman, Y.; Wasserman, E.; Srolovitz, D. J.; Tenne, R. *Science* **1995**, 267, 222.
- (7) Rapoport, L.; Bilik, Y.; Feldman, Y.; Homiyonfer, M.; Cohen, S. R.; Tenne, R. *Nature* **1997**, 387, 791.
- (8) Stephan, O.; Ajayan, P. M.; Colliex, C.; Redlien, Ph.; Lambert, J. M.; Bernier, P.; Lefin, P. *Science* **1994**, 266, 1683.
- (9) Weng-Sieh, Z.; Cherrey, K.; Crespi, V. H.; Cohen, M. L.; Louie, S. G.; Zettl, A. *Phys. Rev. B* **1995**, 51 (11), 229.
- (10) Chopra, N. G.; Luyken, R. J.; Cherrey, K.; Crespi, V. H.; Cohen, M. L.; Louie, S. G.; Zettl, A. *Science* **1995**, 269, 966.
- (11) Mintmire, J. W.; Dunlop, B. I.; White, C. T. *Phys. Rev. Lett.* **1992**, 68, 631.
- (12) Hamada, N.; Sawada, S. I.; Oshiyama, A. *Phys. Rev. Lett.* **1992**, 68, 1579.
- (13) Saito, R.; Fujiata, M.; Dresselhaus, G.; Dresselhaus, M. S. *Appl. Phys. Lett.* **1992**, 60 (18), 2204.
- (14) Odom, T. W.; Huang, J.-L.; Kim, P.; Lieber, C. M. *Nature* **1998**, 391, 62.
- (15) Gao, G.; Çağın, T.; Goddard, W. A., III. *Nanotechnology* **1998**, 9, 184–191.
- (16) Bulusheva, L. G.; Okotrub, A. V.; Romanov, D. A.; Tomanek, D. *J. Phys. Chem. A* **1998**, 102, 975–981.
- (17) Jishi, R. A.; Bragin, J.; Lou, L. *Phys. Rev. B* **1999**, 59 (15), 9862.
- (18) Gülseren, O.; Yildirim, T.; Ciraci, S. *Phys. Rev. B* **2002**, 65 (15), 3405.
- (19) Cote, M.; Cohen, M. L.; Chadi, D. J. *Phys. Rev. B* **1998**, 58, 4277.
- (20) Lee, S. M.; Lee, Y. H.; Hwang, Y. G.; Elsner, J.; Porezag, D.; Frauenheim, Th. *Phys. Rev. B* **1999**, 60, 7788.
- (21) Seifert, G.; Hernandez, E. *Chem. Phys. Lett.* **2000**, 318, 355.
- (22) Marsen, B.; Sattler, K. *Phys. Rev. B* **1999**, 60, 11593.
- (23) Seifert, G.; Kohler, Th.; Urbassek, H. M.; Hernandez, E.; Frauenheim, Th. *Phys. Rev. B* **2001**, 63, 193409.
- (24) Li, B.; Cao, P.; Zhang, R. Q.; Lee, S. T. *Phys. Rev. B* **2002**, 65, 125305.
- (25) Fagan, S. B.; Baierle, R. J.; Mota, R.; da Silva, A. J. R.; Fazzio, A. *Phys. Rev. B* **2000**, 61, 9994.
- (26) Fagan, S. B.; Mota, R.; Baierle, R. J.; Paiva, G.; da Silva, A. J. R.; Fazzio, A. *J. Mol. Struct. THEOCHEM* **2001**, 539, 101–106.
- (27) Zhang, R. Q.; Lee, S. T.; Law, C.-K.; Li, W.-K.; Teo, B. K. *Chem. Phys. Lett.* **2002**, 364, 251–258.
- (28) Kang, J. W.; Seo, J. J.; Hwang, H. J. *J. Nanosci. Nanotech.* **2002**, 2, 6.
- (29) Ivanovskaya, V. V.; Sofronov, A. A.; Ivanovskii, A. L. *Phys. Lett. A* **2002**, 297, 436.
- (30) Singh, A. K.; Kumar, V.; Briere, T. M.; Kawazoe, Y. *Nano Lett.* **2002**, 2 (11), 1243.

- (31) Sha, J.; Niu, J.; Ma, X.; Xu, J.; Zhang, X.; Yang, Q.; Yang, D. *Adv. Mater.* **2002**, *14* (17), 1219.
- (32) Kresse, G.; Hafner, J. *Phys. Rev. B* **1993**, *47*, RC558.
- (33) Kresse, G.; Hafner, J. *Phys. Rev. B* **1996**, *54*, 11169.
- (34) Vanderbilt, D. *Phys. Rev. B* **1990**, *41*, 7892.
- (35) Kresse, G.; Hafner, J. *J. Phys.: Condens. Matter.* **1994**, *6*, 8245.
- (36) Perdew, J.; Wang, Y. *Phys. Rev. B* **1992**, *45*, 13244.
- (37) Kresse, G.; Furthmüller, J. *Comput. Mater. Sci.* **1996**, *6*, 15.
- (38) Wood, D. M.; Zunger, A. *J. Phys. A* **1985**, *18*, 1343.
- (39) Barnard, A. S.; Russo, S. P.; Snook, I. K. *Philos. Mag. B* **2002**, *82*, 1767–1776.
- (40) Barnard, A. S.; Russo, S. P.; Snook, I. K. *Philos. Mag. Lett.* **2003**, *83* (1), 39–45.
- (41) Barnard, A. S.; Russo, S. P.; Snook, I. K. *J. Chem. Phys.* **2003**, *118* (11), 5094–5097.
- (42) Röthlisberger, U.; Andreoni, W.; Parrinello, M. *Phys. Rev. Lett.* **1994**, *72*, 665.